Journal of Environmental Chemical Engineering 8 (2020) 104239

Contents lists available at ScienceDirect

Journal of Environmental Chemical Engineering

journal homepage: www.elsevier.com/locate/jece

Electrochemical enhancement and inhibition of calcium carbonate deposition

Laura Edvardsen[a,*], Kamila Gawel[a], Sigurd Wenner[a], Bartlomiej Gawel[b], Malin Torsæter[a]

[a] Sintef Industry, Trondheim, Norway
[b] Norwegian University of Science andTechnology, Trondheim, Norway

ARTICLE INFO

Editor: P. Giovanni

Keywords:
Scaling
Scaling inhibition
Calcium carbonate
Electrochemically enhanced deposition

ABSTRACT

Calcium carbonate is by far the most widespread scaling material. Its deposition in pipes and flowlines has been a long-standing problem for many industries. Hence, a lot of research is devoted to scale inhibition. One of the calcium carbonate scale management methods relies on removal of calcium ions from scaling solution by electrochemically enhanced deposition. Application of potential between two electrodes may result in oxygen reduction and water electrolysis. Both processes change the local pH in close proximity to the electrodes. Solution close to the anode is becoming acidic while that close to the cathode alkaline. Solubility of calcium carbonate is pH dependent. The alkaline pH in the vicinity of the cathode promotes precipitation of calcium carbonate. On the other hand, the acidic environment near the anode prevents anode from scaling.

In this paper we show how the cathodic and anodic processes, respectively, accelerate and prevent scale deposition on graphite electrode surfaces. The growth of calcium carbonate at different calcium ion concentrations and different voltage magnitudes applied were followed using X-ray computed tomography. The morphology of the deposited calcium carbonate was studied using the scanning electron microscopy. The polymorphic forms of calcium carbonate deposited at different voltage magnitudes were identified using X-ray powder diffraction. A strong correlation between the scaling rate, the average crystallite size and the voltage applied was observed.

1. Introduction

Calcium carbonate is by far the most widespread scaling mineral. Its deposition in pipes has long been a problem for many industries. For example, in oil and gas industry, scale formation may clog wells and pipelines and in extreme cases lead to well shut down. At nuclear power plants, the efficiency of the cooling systems can be severely adversely affected by scale formation [1]. Deposition of calcium carbonate mineral in municipal water supply infrastructure may promote growth of pathogenic bacteria such as e.g. Legionella [2,3]. Hence, a lot of research is devoted to scale inhibition.

The most common scale inhibition is chemical inhibition i.e. use of scale inhibitors - chemicals that retard calcium carbonate precipitation. Application of chemical scale inhibitors, although very popular in oil and gas industry, may not always be acceptable in water supply infrastructure or cooling systems. Therefore, alternative methods have been proposed to prevent or reduce scale formation [2,4]. One of them is removal of calcium ions from scaling solution by electrochemically enhanced deposition of calcium carbonate [2]. Electrochemically enhanced deposition of calcium carbonate was reported by several authors [5–7]. There are two molecular mechanisms underpinning electrochemically enhanced deposition [7]: (i) By applying potential exceeding the water splitting potential to two electrodes, water is electrochemically split. The following reactions take place at anode, Eq. (1), and cathode, Eq. (2). (ii) At potentials below the water splitting potential reduction of oxygen dissolved in water may take place at the cathode as described in Eqs. (3) and (4).

$$6H_2O \rightarrow O_{2(g)} + 4H_3O^+ + 4e^- \quad (1)$$

$$2H_2O + 2e^- \rightarrow H_{2(g)} + 2OH^- \quad (2)$$

$$O_2 + 2e^- + 2H_2O \rightarrow 2OH^- + H_2O_2 \quad (3)$$

$$H_2O_2 + 2e^- \rightarrow 2OH^- \quad (4)$$

All these processes change the local pH close to the electrodes. The pH close to the anode is becoming acidic, while close to the cathode it becomes alkaline [8,9]. During constant voltage (DC, 20 V) electrolysis of water (initial pH 4.5, conductivity 110 μS/cm), the pH at the anode

* Corresponding author.
E-mail address: laura.edvardsen@sintef.no (L. Edvardsen).

https://doi.org/10.1016/j.jece.2020.104239
Received 11 May 2020; Received in revised form 22 June 2020; Accepted 30 June 2020
Available online 02 July 2020

can be reduced to a value of only 3 within a minute. Simultaneously, the pH in the vicinity of the cathode increases to values over 10 [8]. The pH variations in vicinity of the electrodes affect calcium carbonate deposition.

The solubility of calcium carbonate is pH dependent [4]. The generation of hydroxide ions in the vicinity of the cathode leads to increased carbonate ion concentration (CO_3^{2-}) which promotes precipitation of calcium carbonate ($CaCO_3$) according to Eqs. (5) and (6).

$$HCO_3^- + OH^- CO_3^{2-} + H_2O \quad (5)$$

$$Ca^{2+} + CO_3^{2-} \rightarrow CaCO_{3(s)} \quad (6)$$

When calcium ions from the solution precipitate in the form of calcium carbonate at the cathode, the concentration of scaling calcium in the solution decreases. Hence, other surfaces in contact with the solution are protected against scaling, while the cathode acts as a sacrificial material [2,6]. Protection against scaling by reducing the concentration of scaling ions is only one application of electrochemically enhanced deposition (EED), there are several other applications of this process. The EED of calcium carbonate has also been proposed as a method for creating artificial reefs [10,11]. This concept relies on growing calcium and magnesium carbonates on a metal scaffold placed in seawater. By applying potential between the conductive scaffold and a sacrificial electrode, the growth of carbonates is facilitated, and an artificial reef is formed. The cathodic deposition of calcium carbonate has also been utilized in corrosion protection of metal surfaces [12]. During cathodic processes both high pH close to cathodes as well as the formation of isolating mineral layers protect metal surfaces from corrosion. The cathodic deposition of carbonate minerals has also been suggested as a carbon sequestration method [13]. Despite of many practical applications, the cathodic deposition of calcium carbonate and other minerals may have negative impact on many electrochemical processess. One example could be deactivation of biocathode in a microbial fuel cell [14,15].

While the cathodic processes are used to enhance calcium carbonate precipitation, the anodic reactions have been utilized in scaling prevention [16]. One example of electrochemical scaling prevention has been described by Duan et al. (2014). Reverse osmosis membranes made of polyamide and carbon nanotubes were in their work shown to retard $CaCO_3$ and $CaSO_4$ scaling upon intermittent application of a 2.5 V potential to the membrane surface, when the membrane acted as an anode. Electrochemical dissolution of calcium carbonate has also been suggested as a solution for mitigating carbon dioxide induced ocean acidity [17].

During calcium carbonate electrochemical deposition at constant potential, the residual current density is proportional to the electrode surface area and it decreases when the active surface area decreases. The residual current density reaches a value close to zero when the surface is completely covered by calcium carbonate, causing the deposition to cease. According to Hui and Ledion [18], the morphology of calcium carbonate deposits and their porosity is related to the residual current. It is also related to the nature of the substrate. A strong correlation exists between the rate of nucleation and the crystal polymorph [19]. The nucleation rate depends on the nature of the substrate [20]. It was shown that the presence of a passivating layer on non-noble metals reduces the density of nucleation sites and thus promotes the formation of vaterite nuclei [19]. Further growth of aragonite crystals involves a total phase transformation from vaterite nuclei into aragonite [19].

The main objective of this work were to: (a) study the growth of calcium carbonate on graphite electrodes, (b) compare calcium carbonate growth at the cathode, anode and reference rods, (c) find the relation between potential and growth rate as well as morphology of the precipitated calcium carbonate, (d) identify polymorphic form(s) of the resulting deposits in each of the cases.

2. Materials and methods

2.1. Electrochemical deposition of calcium carbonate

Electrochemical deposition of calcium carbonate was induced by applying potential between two graphite electrodes immersed in a scaling solution. The scaling solutions studied contained 0.15 and 1.5 wt% $CaCl_2$. The pH of the scaling solution was adjusted to 12 using NaOH right before the onset of the experiment (not longer than 30 min). Three cylindrical graphite rods, with a diameter of 2.8 mm, were immersed in the scaling solution after their surfaces were cleaned with isopropanol. Two rods were connected to a power supply and acted as a cathode and an anode, while the third graphite rod was a reference. All three graphite rods were immersed in 900 mL of $CaCl_2$ solution. The distance between the cathode and the anode was approximately 7 cm in each experiment, while the reference was placed at a considerable distance from the electrodes. The scaling was induced by introducing gaseous CO_2 to the solution by bubbling. The CO_2 gas flow rate was 5.64 mL/min in each of the experiments. When the CO_2 injection hose was immersed in the solution, the power supply was switched on, and the potential between cathode and anode was applied. Experiments were conducted at 10, 5, 3 and 1 V. The series of experiments was performed in a fume hood at room temperature (23 °C) and atmospheric pressure and carried out for 6 h in total. Every hour the electrodes and the reference rod were removed from the scaling solution and quenched by a quick (1 s) immersion in deionized water. This was done to remove the excess of ions, and thus prevent crystallization of the remaining salts during the following drying process. The rods were further scanned using X-ray micro-computed tomography (μ-CT). The scaling solution was renewed every 1 h.

The evolution of pH and conductivity during the experiment was followed using WTW inoLab®, Multi 9630 IDS multimeter equipped with pH sensor (SenTix® Micro 900-P) and conductivity sensor (TetraCon®,925). The results are presented in Fig. 1. At time 0 the hose with the CO_2 distributor (attached in order to allow for homogeneous distribution of CO_2 gas) was placed in the solution and any changes in the pH were registered. The pH and conductivity measurements were made by inserting the sensors in between the two electrodes.

2.2. X-ray micro-computed tomography (μ-CT)

X-ray micro-computed tomography (μ-CT) was performed using an industrial CT scanner (XT H 225 ST). It was operated at 210 kV and with a current of 155 μA. A tin filter was used. The raw CT data were reconstructed into cross sectional slices.

Avizo Fire software (version 9.1, FEI, 2016) was used to estimate the volume ratio between the precipitated calcium carbonate and the graphite. During segmenting, the sections of each of the materials were selected by thresholding based on image intensities. Thereafter, the material volumes were calculated for the chosen section of the rod. In order to find out to what extend the segmentation affacts the volume estimates, the segmentation was performed twice for the lowest and highest exposure times. The maximum error in estimating volume ratios was calculated to be 1 %.

2.3. Scanning electron microscopy (SEM)

1 cm pieces of the precipitated material were broken off from the middle of the electrodes for scanning electron microscopy (SEM) imaging of the surface. A Hitachi S3400 N thermal emission microscope was used in low-vacuum mode (20 Pa pressure) to prevent static charging of calcium carbonate. The acceleration voltage was set to 15 kV and the working distance was 6 mm. A backscattered electron (BSE) detector was used in 3D mode to optimize topographic contrast in the SEM images.

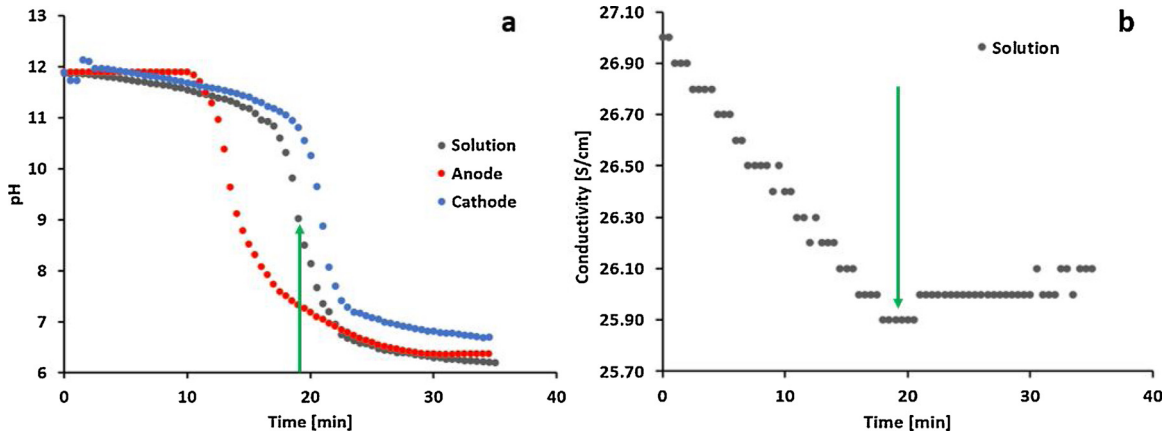

Fig. 1. Time evolution of pH (a) and conductivity (b) in a 1.5 wt% $CaCl_2$(aq) solution with graphite electrodes polarized at 5 V. The bulk solution is represented in grey, while red and blue indicate the solution adjacent to the anode and cathode, respectively. (For interpretation of the references to colour in this figure legend, the reader is referred to the web version of this article).

2.4. Powder X-ray diffraction (XRD)

In order to identify the polymorphic form of the deposited calcium carbonate, powder X-ray diffraction was used. The samples for XRD measurements were prepared by removing the precipitate from the graphite rod and thereafter grinding the material by hand using a mortar and pestle. The measurements were performed at room temperature, between 10 and 75° 2θ on a Bruker D8 Advance DaVinci diffractometer with Bragg-Brentano geometry using CuK_α radiation (λ = 1.54187 Å). The X-ray powder diffraction pattern was collected over the course of one hour.

3. Results and discussion

Fig. 1 displays the time evolution of pH and conductivity in the 1.5 wt% $CaCl_{2(aq)}$ solution mid-way between electrodes (~3.5 cm from electrode surface). The figure also shows measurements in the solution at a distance of around 4 mm from cathode and anode (polarized at 5 V). Initially, the pH of the $CaCl_2$ solution is brought to a value of 12 by addition of sodium hydroxide. At time 0, the solution gets in contact with CO_2. The CO_2 then reacts with water according to Eq. (7) and forms carbonic acid. At the initially high pH,12, carbonic acid molecules tend to dissociate almost entirely to form hydrogen and carbonic ions according to Eq. (8). The products in Eq. (8) further react with hydroxide ions and calcium ions present in the solution according to Eqs. (9) and (10), respectively. As a result of the reaction in Eq. (9), the pH value of the solution is reduced, while the reaction in Eq. (10) leads to precipitation of scarcely water-soluble calcium carbonate.

$$CO_2 + H_2O \rightleftarrows H_2CO_3 \quad (7)$$

$$H_2CO_3 \rightleftarrows 2H^+ + CO_3^{2-} \quad (8)$$

$$2Na^+ + 2OH^- + 2H^+ + CO_3^{2-} \rightarrow 2H_2O + 2Na^+ + CO_3^{2-} \quad (9)$$

$$Ca^{2+} + 2Cl^- + 2H^+ + CO_3^{2-} \rightarrow CaCO_3\downarrow + 2Cl^- + 2H^+ \quad (10)$$

The pH in the vicinity of the anode was observed to decrease faster compared to in the bulk solution and at the cathode. This was due to the electrochemical processes taking place at the anode described in Eq. (1). More precisely, this is a result of the production of hydrogen ions that contribute to faster neutralization of the alkaline pH. On the other hand, the pH at the cathode decreased more slowly compared to bulk and at the anode. This was because of production of hydroxide ions that counteracted the effect of carbonic acid. Moreover, it contributed to increasing the pH in the solution. A pH value of 10 was thus reached 6.5 min faster on the anode than on the cathode. Moreover, the pH value 4 mm away from the cathode was sustained at higher values compared to anode and bulk solution after the pH had decreased below 7. It is expected that pH profiles measured even closer to the electrode surface would have a larger time-shift than what is seen in our measured profiles.

Conductivity values in the solution decreased linearly from the initial value of 27 S/cm to the minimum value of 25.9 S/cm within around 20 min from the reaction onset. The decrease is due to the consumption of calcium, hydrogen and carbonate ions according to Eqs. (9) and (10). It can be assumed that after 20 min of the reaction, an equilibrium amount of calcium ions was consumed and precipitated in the form of water insoluble calcium carbonate. The further slight increase in conductivity, to the value of 26.1 S/cm after 35 min, can possibly be attributed to the increasing concentration of hydrogen ions, Eq. (8), as well as calcium ions that are not consumed in hydroxide neutralization, Eq. (9), or calcium carbonate precipitation, Eq. (10).

When graphite rods are immersed in the $CaCl_2/CO_2$ scaling solution, calcium carbonate precipitates on their surfaces. Depending on the polarity of the electrode either enhancement or inhibition of scaling may take place. More precisely, the acceleration of calcium carbonate deposition compared to the reference electrode was observed at the negative electrode (cathode) while inhibition at the positive electrode (anode). Fig. 2 compares surfaces of cathode, anode and the reference rod after 2 h of exposure to scaling solution (1.5 wt% $CaCl_2$) with 5 V potential between electrodes. While the surface of the reference rod is slightly covered with white precipitate, the surface of the cathode is entirely covered with a thick layer of calcium carbonate. In contrast to the cathode and reference rod, the anode is free of precipitate. The observation suggests that the negative polarization accelerates deposition of calcium carbonate while the positive inhibits it. The mechanisms

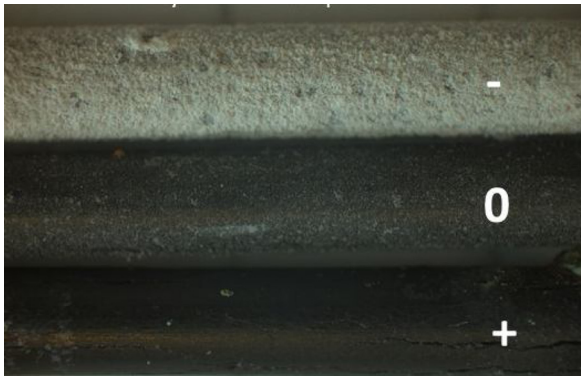

Fig. 2. Graphite electrodes: cathode (top), reference (middle) and anode (bottom) after 2 h in 1.5 wt% $CaCl_2$ solution at 5 V.

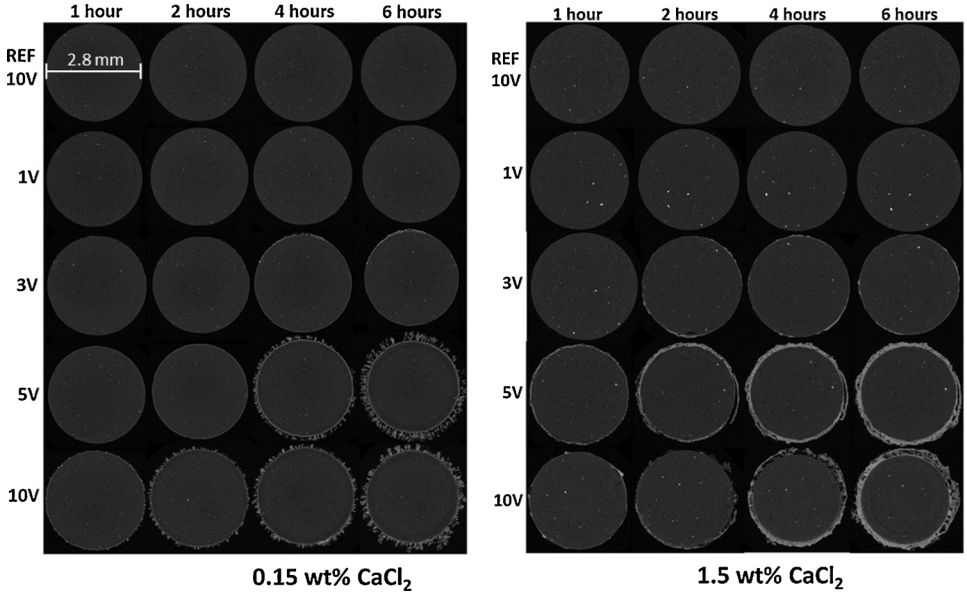

Fig. 3. μ-CT scans of graphite cathodes and reference rods exposed to different concentrations of $CaCl_2$ solution, 0.15 wt% (left) and 1.5 wt% (right), and at different potentials.

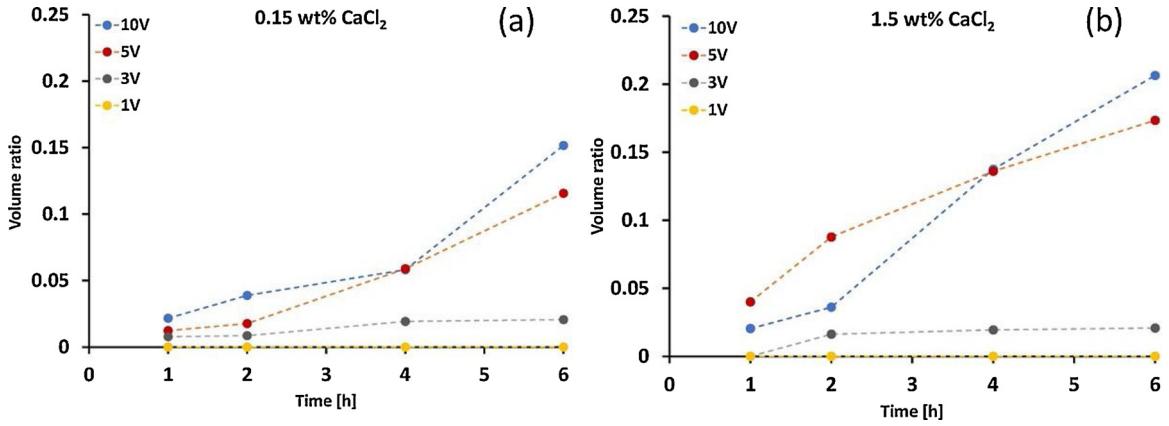

Fig. 4. The volume ratio between calcium carbonate precipitate and the graphite rod (CC/G) as a function of time for different potentials in 0.15 wt% (a) and 1.5 wt% (b) $CaCl_2$ solutions. The segmentation errors were typically smaller than 1 %. The errer bars were thus smaller than indicators which is why they are not shown on the plot.

underlying acceleration and inhibition of calcium carbonate deposition are related to the local pH close to the electrode surfaces. The local pH close to the cathode is alkaline, which is associated with reduction of hydrogen and generation of hydroxide ions according to Eqs. (2)–(4). On the other hand, the local pH close to the anode is acidic due to oxidation of oxygen described by Eq. (1). The precipitation of calcium carbonate is pH sensitive and take place spontaneously at alkaline conditions, while acidic conditions prevent it [4]. Thus, the surface of the cathode (alkaline) was covered with a thick layer of calcium carbonate precipitate after 2 h of exposure to the scaling solution, and the anode was prevented from calcium carbonate deposition. The inhibition of scale deposition at the anode is in line with the study reported by Duan et al. (2014) who applied polarization to reverse osmosis membranes containing conductive carbon nanotubes to prevent the membrane from scaling [16]. The authors show that upon intermittent application of a 2.5 V potential to the membrane surface, the $CaCO_3$ and $CaSO_4$ scaling is retarded when the membrane acts as an anode.

The growth of calcium carbonate deposition on graphite cathodes was studied using X-ray computed tomography (CT) at different calcium chloride concentrations and potentials, at constant CO_2 flow. Fig. 3 shows the CT cross-sections through the graphite cathodes and reference rods after 1, 2, 4 and 6 h of exposure to the scaling solutions (0.15 wt% and 1.5 wt% of $CaCl_2$). The dark grey circles are the solid graphite rods, while the brighter rim at the surfaces is the calcium carbonate precipitate. No precipitate was observed at the graphite surfaces within 6 h for the reference rod and for the cathode at 1 V. After 4 h in 0.15 wt% $CaCl_2$ solution, and after 2 h in 1.5 wt% $CaCl_2$ solution, a thin film of calcium carbonate was observed at the surface of the cathode polarized at 3 V. For 5 V polarization, a thin film of precipitate was observed already after 2 h in 0.15 wt% $CaCl_2$ solution and after 1 h in 1.5 wt% $CaCl_2$ solution. At 10 V, precipitate was observed for both solutions already after the first hour of exposure. The low concentration (0.15 wt% $CaCl_2$) solution supported precipitation of fractal-shaped features growing from the graphite surface, while the precipitate at high concentration (1.5 wt% $CaCl_2$) had a more homogeneous morphology and formed a porous layer. The porosity of the layer was higher when higher potentials were applied. The precipitated layer on the reference rods were too thin to be observed on the CT images, but was nonetheless present, as seen from Fig. 2.

The volume ratio between calcium carbonate precipitate and the graphite rod (CC/G) was estimated by the procedure described in the *Materials and Methods* section. The CC/G volume ratio is plotted vs.

exposure time for the two scaling solutions (0.15 wt% and 1.5 wt% of $CaCl_2$) in Fig. 4. It suggests that the optimal conditions for calcium carbonate electrochemically enhanced precipitation were reached at 5 V. At 3 V precipitation was slow in both solutions while at 10 V some losses of deposited calcium carbonate layer were encountered. The losses were due to erosive processes associated with intense gas release ($H_{2(g)}$; see Eq. (2)), which led to fragments of calcium carbonate being torn off the sample, thus lowering the CC/G ratio. These occurrences happened at random time intervals, and explains why the CC/G ratio is often lower compared to the values obtained at 5 V. It is likely that the volume ratio for 10 V would have been much higher than at 5 V if no calcium carbonate had been lost during the experiment. This suggest that 10 V is less favourable for electrochemical precipitation on a graphite electrode than 5 V. The CC/G ratio after 6 h for 5 and 10 V was higher at 1.5 wt% of $CaCl_2$ compared to 0.15 wt%.

The plots for 3 and 5 V follow a s-shaped/sigmoidal profile. The characteristic feature of sigmoidal profile is that rates are low at the beginning and at the end of the deposition but rapid in between. This behavour is clearly seen for 3 V. The initial slow rates can be attributed to the time required for a significant number of nuclei of the calcium carbonate to form at the surface and begin growing. During the intermediate period, the transformation is fast. The crystallites grow faster and and nuclei continue to form on the surface. The slowdown at the later stage may in our case be caused by the decrease of the electrochemically active surface area due to non-conductive calcium carbonate deposition. The s-shaped curve is characteristic for Johnson–Mehl–Avrami–Kolmogorov crystallization model [21]. The Avrami equation, see Eq. (11), expresess the fraction of transformed material (θ) after a reaction time (t) at a given temperature.

$$\theta = 1 - \exp(-K(t)^n) \tag{11}$$

The Avrami equation can be also expressed as

$$\ln(\ln(1/(1-\theta(t)))) = \ln K + n \ln t \tag{12}$$

where:

$$K = \pi N G^3/3$$

N is the nucleation rate per unit volume

G is the growth velocity of a crystal

n = D + 1 where D is the dimensionality of space in which crystallization occurs for uniform nucleation and growth

The data from 3 and 5 V presented in Fig. 4 were used to derive deposition kinetics and to fit Avrami crystallization model. The data for 1 V and 10 V were discarded due to low deposition or partial loss of calcium carbonate deposit respectively. The calcium carbonate volumes obtained from CT scans were recalculated to the mole fraction of calcium deposited on the surface in respect to the total amount of calcium initially present in the solution (θ). The fits are presented in Fig. 5. The Avrami model gave a good fit to the experimental data which allowed for the determination of the constants n (slope) and lnK (intercept) from a plot of ln ln(1/(1 − θ)) versus ln t, see Fig. 5. The low values of n suggest that the crystallites growth is restricted in respect to dimensions. Values of 1 can be expected for crystallites growing on surfaces [22] which is the case here.

Fig. 6 presents SEM BSE images showing the topography of calcium carbonate deposited at the graphite surface after 6 h of deposition from 1.5 wt% $CaCl_2$ solution at different potentials (1, 3, 5, 10 V) and from 0.15 wt% $CaCl_2$ solution (LC) at potentials 5 and 10 V. The surface of the cathode polarized at the potential of 1 V is only partially covered with calcium carbonate and large areas of graphite remained uncovered. At the potential of 1 V, water splitting is not favoured at the electrode surfaces and only reduction of oxygen dissolved in water may contribute to increased pH at the cathode according to Eqs. (3) and (4). Graphite surfaces polarized at 3, 5 and 10 V were entirely covered with calcium carbonate. The crystallite size increased with polarization potential, and was highest at 10 V. Calcium carbonate crystallites deposited from low concentration (0.15 wt%) were more homogeneously distributed over the surface and were smaller compared to those deposited at higher concentration (1.5 wt%), see Fig. 6.

Fig. 7 shows typical crystallite sizes and forms of calcium carbonate crystallites deposited at different polarization voltages and at different concentrations. At the surface polarized at 1 V, the most common crystallite structure was spherical and spherulitic crystallites in the size ranging between 2 and 4 μm. At 3 V the 4–6 micrometer large spherulites were present at the surface of prism-like crystallites. At higher potential, the prism-like crystallites were more abundant, and the number of spherulites at their surface was lower.

X-ray diffraction indicated that calcite was the only polymorphic form of calcium carbonate deposited on the surface of graphite. The diffraction patterns presented in Fig. 8 indicate the presence of peaks characteristic for calcite for all polarization potentials. This suggests that the changes in polarization potential do not affect the polymorphic form of the electrodeposited calcium carbonate. This also suggests that the observed spherical and spherulitic crystallites may be calcite. The literature reports spherical calcite crystallites [23], however, the most commonly reported are vaterite spheres and spherulites [24,25]. It is likely that the spherical forms of vaterite, if present, are only at the surface at low content with respect to the bulk calcite material which might have been undetected by XRD measurements. It has been suggested that vaterite phase may be a precursor form of hydrated calcium carbonate and also that it is not a stoichiometric $CaCO_3$ phase; rather, a Ca-rich material with small incorporations of (OH), HCO_3, or CO_2 (aq.) [25]. This could explain why the spherical structures are present only at the very external surface, but not further in the bulk material as they

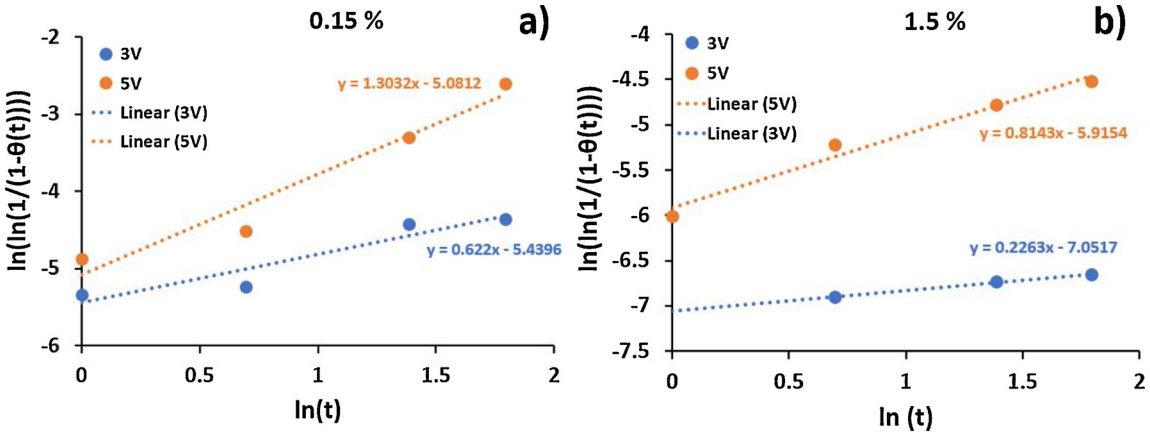

Fig. 5. Avrami crystallization model fitted to the experimental data from Fig. 4.

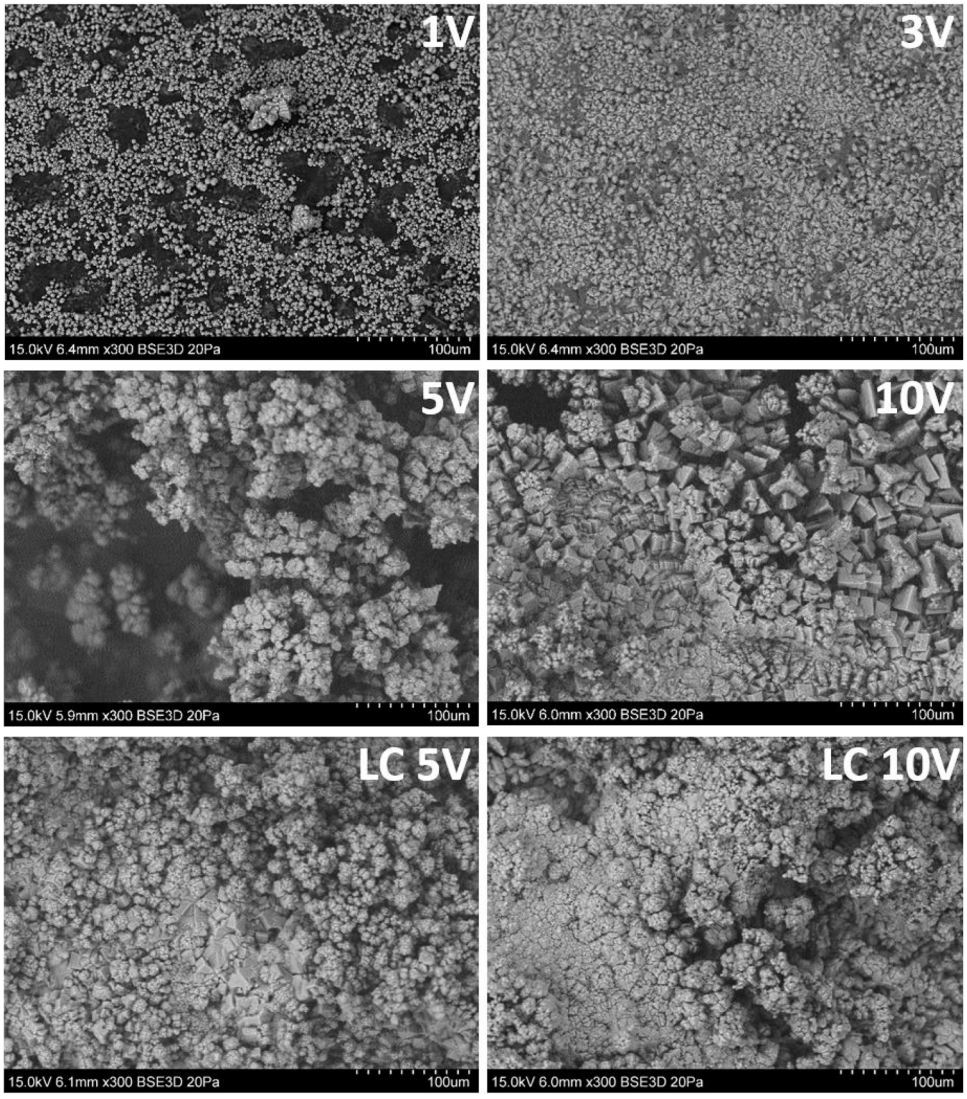

Fig. 6. SEM BSE images presenting topography of calcium carbonate deposited at graphite surface after 6 h of deposition from a 1.5 wt% $CaCl_2$ solution at different potentials (1, 3, 5, 10 V) and a 0.15 wt% $CaCl_2$ solution (LC) at potentials 5, 10 V.

constitute a transitional and unstable form of calcium carbonate that at later stages tends to recrystallize to the most stable calcite [26]. The presented diffraction patterns are normalized in respect to the highest peak. The intensity differences observed between peaks may indicate that the calcite crystallites grow with a preferred orientation.

4. Conclusions

In this paper we show how scale deposition on graphite surfaces can be accelerated and prevented by cathodic and anodic processes, respectively. The mechanisms underpinning the scale deposition acceleration at the cathode, and inhibition at the anode, have been outlined. The acceleration and inhibition reactions are both driven by changes in the local pH close to the electrode surfaces. Growth of calcium carbonate deposition at different calcium ion concentrations and different polarization potentials applied were studied using X-ray computed tomography. In the paper we demonstrate that by increasing the polarization potential between electrodes, the deposition rate grows to a certain threshold, above which erosive processess tear off deposited calcium carbonate from the surface. The increasing polarization potential also results in increased crystallite sizes, and it promotes deposition of prism-like crystallites at the surface instead of the spherulitic shapes observed at low potentials. Polymorphic forms of the deposited calcium carbonate was not affected by the polarization potential.

Both cathodic and anodic processes can be utilized in scale prevention. While the enhanced deposition at the cathode may be utilized to reduce the concentration of the scaling mineral in the scaling solution, the inhibition at the anode may be directly applied for preventing surfaces from scaling. The anodic inhibition is, however, limited to the surfaces that will not undergo galvanic corrosion at the choosen conditions.

CRediT authorship contribution statement

Laura Edvardsen: Conceptualization, Methodology, Investigation, Writing - original draft, Writing - review & editing. **Kamila Gawel**: Conceptualization, Methodology, Investigation, Writing - original draft, Writing - review & editing. **Sigurd Wenner**: Formal analysis, Writing - review & editing. **Bartlomiej Gawel**: Formal analysis, Writing - review & editing. **Malin Torsæter**: Funding acquisition, Conceptualization, Project management, Writing - review & editing.

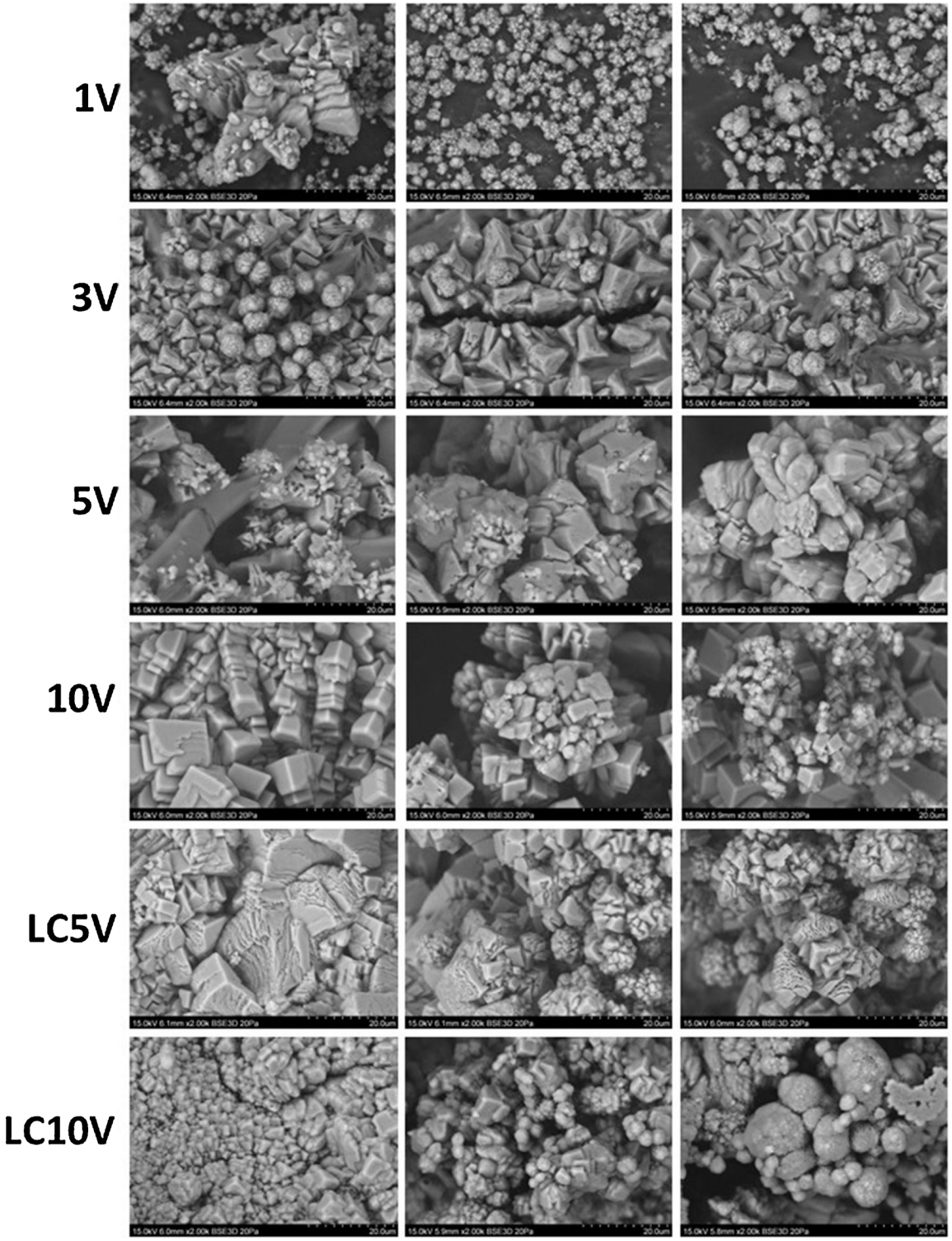

Fig. 7. SEM BSE images of characteristic calcium carbonate crystal morphologies present at the surface after 6 h of deposition from a 1.5 wt% $CaCl_2$ solution at different potentials (1, 3, 5,10 V) and a 0.15 wt% $CaCl_2$ solution (LC) at potentials 5 and 10 V.

Declaration of Competing Interest

The authors declare that they have no known competing financial interests or personal relationships that could have appeared to influence the work reported in this paper.

Acknowledgements

The authors gratefuly acknowledge the financial support from The Norwegian Research Council in the form of grant number 285568 "Well fossilization for P&A" and from the strategic SINTEF Industry project number 102021203 "Electrophoretic cleaning and friction reduction for applications in drilling and well construction". The use of the X-ray laboratory at NTNU as well as the kind assistance of the laboratory

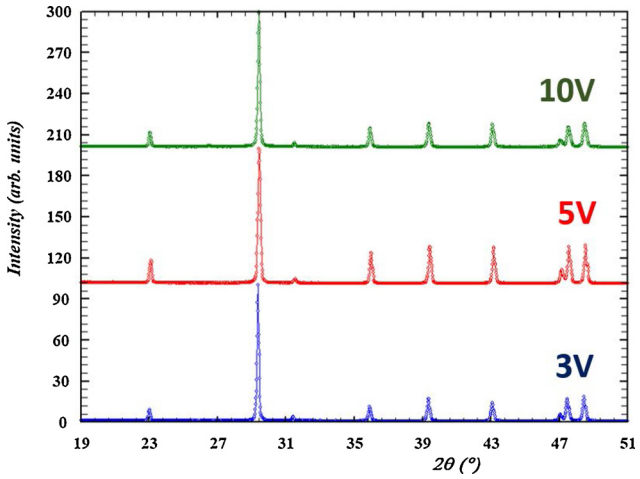

Fig. 8. XRD patterns for calcium carbonate material deposited at the surface of the cathode polarized at 10 V (top), 5 V (middle) and 3 V(bottom), showing identical peak positions characteristic of calcite [27].

engineer Ole Tore Buset is gratefully acknowledged. The authors wish to extend their special thanks to Dr Alexandre Lavrov for valuable discussions and comments on the article.

References

[1] C. Gabrielli, et al., Study of calcium carbonate scales by electrochemical impedance spectroscopy, Electrochim. Acta 42 (8) (1997) 1207–1218.
[2] A. Dirany, P. Drogui, M.A. El Khakani, Clean electrochemical deposition of calcium carbonate to prevent scale formation in cooling water systems, Environ. Chem. Lett. 14 (4) (2016) 507–514.
[3] M. Koubar, M.H. Rodier, J. Frere, Involvement of minerals in adherence of Legionella pneumophila to surfaces, Curr. Microbiol. 66 (5) (2013) 437–442.
[4] P. Hart, G. Colson, J. Burris, Application of carbon dioxide to reduce water side lime scale in heat exchanges, J. Sci. Technol. For. Prod. Process. 1 (2012) 67–70.
[5] A.R. Rakitin, V.I. Kichigin, Electrochemical study of calcium carbonate deposition on iron. Effect of the anion, Electrochim. Acta 54 (9) (2009) 2647–2654.
[6] C. Gabrielli, et al., Nucleation and growth of calcium carbonate by an electrochemical scaling process, J. Cryst. Growth 200 (1) (1999) 236–250.
[7] H. Karoui, et al., Electrochemical scaling of stainless steel in artificial seawater: role of experimental conditions on CaCO3 and Mg(OH)2 formation, Desalination 311 (2013) 234–240.
[8] James H. Dickerson, A.R.B, Electrophoretic Deposition of Nanomaterials, Springer Science & Business Media, 2011.
[9] C. Deslouis, I. Frateur, G. Maurin, B. Tribollet, Interfacial pH measurement during the reduction of dissolved oxygen in a submerged impinging jet cell, J. Appl. Electrochem. 27 (4) (1997) 482–492.
[10] P. van Treeck, H. Schuhmacher, Artificial reefs created by electrolysis and coral transplantation: an approach ensuring the compatibility of environmental protection and diving tourism, Estuar. Coast. Shelf Sci. 49 (1999) 75–81.
[11] W. Hilbertz, D. Fletcher, C. Krausse, Mineral accretion technology: applications for architecture and aquaculture, Ind. Forum 8 (4–5) (1977) 75–84.
[12] P. Pedeferri, Corrosion Science and Engineering, (2018).
[13] C. Carré, et al., Electrochemical calcareous deposition in seawater. A review, Environ. Chem. Lett. (2020).
[14] M. Santini, et al., Carbonate scale deactivating the biocathode in a microbial fuel cell, J. Power Sources 356 (2017) 400–407.
[15] M. Santini, et al., Three-dimensional X-ray microcomputed tomography of carbonates and biofilm on operated cathode in single chamber microbial fuel cell, Biointerphases 10 (3) (2015) 1–9.
[16] W. Duan, et al., Electrochemical mineral scale prevention and removal on electrically conducting carbon nanotube – polyamide reverse osmosis membranes, Environ. Sci. Process. Impacts 16 (6) (2014) 1300–1308.
[17] G.H. Rau, Electrochemical splitting of calcium carbonate to increase solution alkalinity: implications for mitigation of carbon dioxide and ocean acidity, Environ. Sci. Technol. 42 (23) (2008) 8935–8940.
[18] F. Hui, J. Lédion, Evaluation methods for the scaling power of water, Eur. J. Water Qual. 33 (2002) 41–52.
[19] C. Gabrielli, et al., Study of the electrochemical deposition of CaCO3 by in situ Raman spectroscopy: I. Influence of the substrate, J. Electrochem. Soc. 150 (7) (2003) C478–C484.
[20] M. Euvrard, et al., Kinetic study of the electrocrystallization of calcium carbonate on metallic substrates, J. Cryst. Growth 291 (2006) 428–435.
[21] M. Avrami, Kinetics of phase change. I. General theory, J. Chem. Phys. 7 (12) (1939) 1103.
[22] J.W. Cahn, Transformation kinetics during continuous cooling, Acta Metall. 4 (6) (1956) 572–575.
[23] S.L. Tracy, C.J.P. François, H.M. Jennings, The growth of calcite spherulites from solution: I. Experimental design techniques, J. Cryst. Growth 193 (3) (1998) 374–381.
[24] A.J. Easton, D. Claugher, Variations in a growth form of synthetic vaterite, Mineral. Mag. 50 (356) (2018) 332–336.
[25] J.W. McCauley, R. Roy, Controlled nucleation and crystal growth of various CaC03 phases by the silica gel technique, Am. Mineral. 59 (9-10) (1974) 947–963.
[26] R.A. Boulos, et al., Spinning up the polymorphs of calcium carbonate, Sci. Rep. 4 (1) (2014) 3616.
[27] R.W.G. Wyckoff, The crystal structures of some carbonates of the calcite group, Am. J. Sci. (50) (1920) 317–360 Serie 4(-1920).